

## Correspondence

### *Etching channels and grain-boundary grooves on ice surfaces in the scanning electron microscope*

It is important to locate the intersection of a grain boundary with an ice surface when interpreting micrographs of polycrystalline ice obtained from the scanning electron microscope (SEM). This is because if the boundary's location on the surface is not known accurately one cannot easily draw conclusions regarding the whereabouts of impurities within the structure (Barnes and others, 2003). Previously we have (Barnes and Wolff, 2004) presented an image (reproduced here; Fig. 1a) showing the etch channel, formed on an ice surface subliming under vacuum, which does not match the location of the narrower etch channel within a bubble cavity. We suggested that the rate of sublimation (etching) within the bubble cavity was less than the rate on the specimen surface due to the curvature of the bubble. Consequently, while the channel within the bubble could be used to approximate the location of the grain-boundary–surface intersection, the etch channel on the more rapidly subliming surface could not be used in this way. We interpreted this etching channel as being formed, not as a direct result of the location of the grain boundary on the surface during etching, but due to the morphology of the grain-boundary groove originally present on the ice prior to sublimation under vacuum. Thus the intersection of the grain boundary with the ice surface is not necessarily co-located with the position of the etching channel if the grain boundary is angled obliquely to the surface.

Recently Obbard and others (2006) suggested that the lack of intersection on the micrograph (Fig. 1a) was an optical illusion resulting from an artefact of the secondary electron detector. To support this assertion they presented micrographs of the intersection between two aluminium blocks with hemispherical dimples milled at the boundary, and a thermodynamic argument regarding rates of sublimation from surfaces and grain boundaries. They also presented images of etched polycrystalline ice surfaces which clearly showed differing crystalline orientations in neighbouring grains backed up with impressive backscattered electron diffraction measurements. While we agree that an apparent mismatch between grain boundaries and

etching grooves at the specimen surface can be generated through an imaging artefact, we can provide further evidence to support our earlier interpretation of our image.

In order to clarify the discussion, we need first to explain the different treatments that may be applied to an ice surface. In the experiments of Obbard and co-workers, as well as Barnes and co-workers, flat ice surfaces are first prepared by cutting a sample with a microtome knife (or hand-held razor blade in the former case) at warm temperatures (typically  $-20^{\circ}\text{C}$ ). The sample may then be taken to liquid nitrogen temperatures immediately, in which

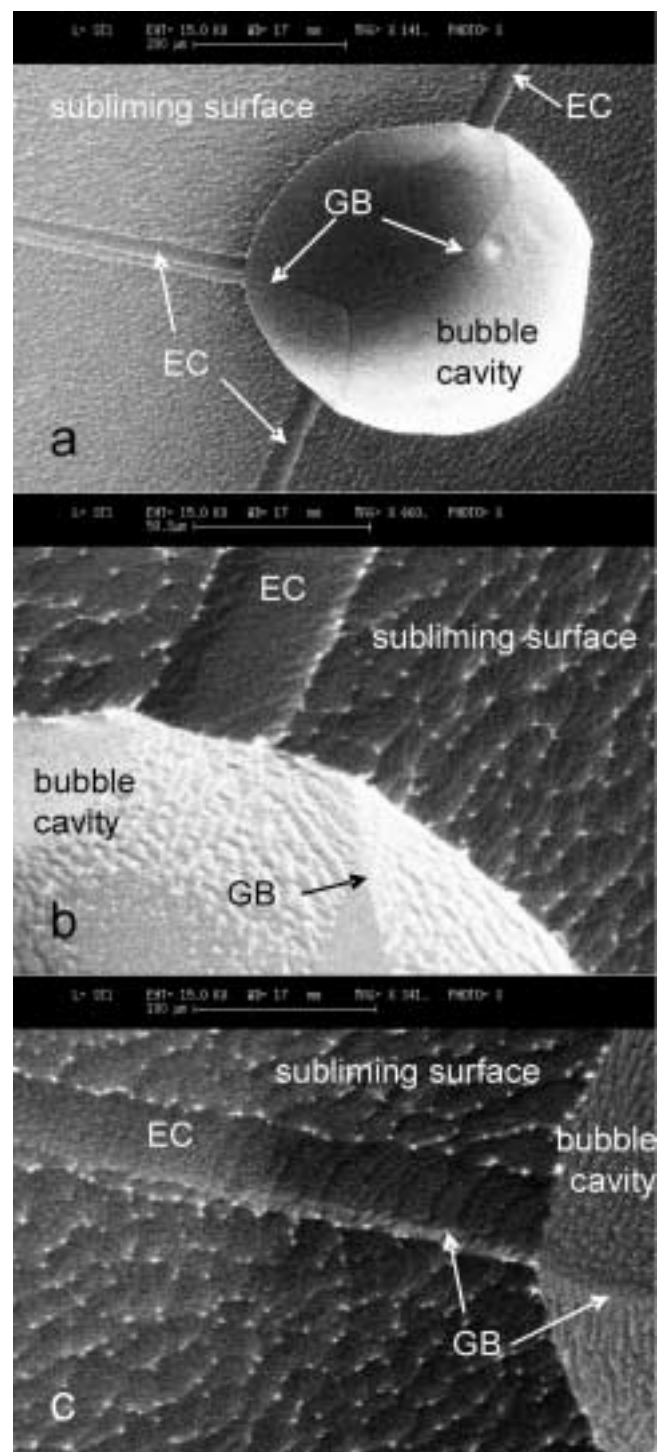


**Fig. 1.** (a) The intersection of the subliming surface of ice from Dome C, Antarctica, with an air bubble, showing etching channels on the surface and in the bubble cavity which probably approximate the location of grain boundaries. The surface has been sublimed at  $-70^{\circ}\text{C}$  under vacuum for 10 min at a rate of  $\sim 20\mu\text{m min}^{-1}$ . Reproduced from Barnes and Wolff (2004); note the mismatch between the surface etching channels (EC) and the grain boundaries (GB) at the top and bottom of the bubble. The left side of the bubble shows a GB coincident with the EC forming a ridge. (b) The intersection of the grain boundary in the bubble cavity with the subliming surface shown at the top of (a) after 13 min at  $-70^{\circ}\text{C}$  under vacuum. There is no grain boundary apparent on the subliming surface; the etch channel appears to be offset from the channel in the bubble cavity. (c) The intersection at the left side of the bubble cavity after 19 min at  $-70^{\circ}\text{C}$  under vacuum. The ridge thought to result from collection of impurities at the grain boundary is now located just at the bottom edge of the etching channel.

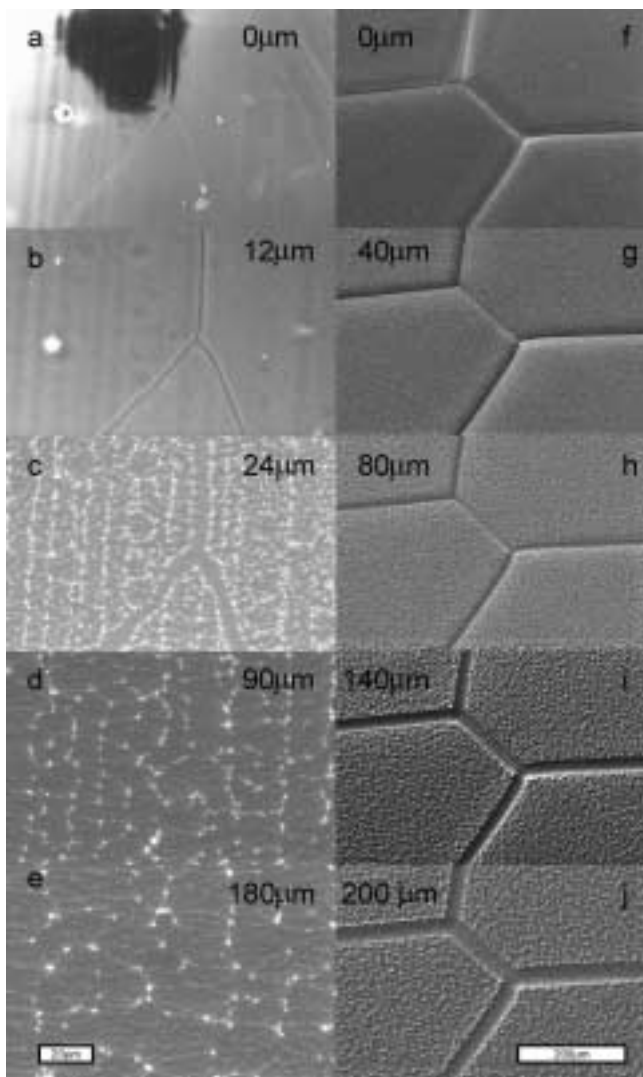


**Fig. 2.** (a) Greenland ice surface showing a triple junction of grain boundaries (dark area is due to surface charging). The specimen was cut in a cold room at  $-20^{\circ}\text{C}$  and then transferred in less than 5 min to the SEM at  $-196^{\circ}\text{C}$ ; the width of the grain-boundary groove is  $1\text{--}2\ \mu\text{m}$ . (b–e) Surface shown in (a) (at the same magnification) during sublimation at  $-80^{\circ}\text{C}$  under vacuum; the etching rate is estimated to be  $6\ \mu\text{m}\ \text{min}^{-1}$ . The depth of ice sublimated from the surface is shown in each panel. The location and boundaries of the etch channel are no longer discernible after 30 min. (f) Dome C ice surface showing two triple junctions and grain boundaries. The specimen was cut in a cold room at  $-20^{\circ}\text{C}$  and left to stand for 3 days followed by transfer to the SEM at  $-196^{\circ}\text{C}$ . The width of the groove is  $\sim 25\ \mu\text{m}$ . (g–j) Surface shown in (f) (at the same magnification) during sublimation at  $-70^{\circ}\text{C}$  under vacuum; the etching rate is estimated to be  $20\ \mu\text{m}\ \text{min}^{-1}$ . The depth of ice sublimated from the surface is shown in each panel. The location of the etch channel is clearly discernible after 10 min of etching. Note the difference in scale bars between figures (a–e) and (f–j).

case the sample appears flat, except for cutting artefacts, with no significant grain-boundary groove. In other cases, the sample may be left at a warm temperature at atmospheric pressure for some time before cooling; in this case, clear grain-boundary grooves are formed, and we refer to this as ‘pre-etching’. After either treatment, the sample may be warmed from liquid nitrogen temperatures on the cold stage of the SEM; this process, which we call ‘etching’, leads to sublimation under vacuum.

The specimen in question (Fig. 1a) was pre-etched for 1 day at  $-20^{\circ}\text{C}$  at atmospheric pressure to form grain-boundary grooves, prior to insertion into the SEM at  $-196^{\circ}\text{C}$  and the subsequent sublimation at  $-70^{\circ}\text{C}$  for 10 min at a rate of  $\sim 20\ \mu\text{m}\ \text{min}^{-1}$ , to reveal the surface shown. The experimental details are described elsewhere (Barnes and others, 2002). Figure 1b shows the top intersection after 13 min of etching. The ‘grain-boundary’ channel within the bubble cavity still does not appear coincident with the etching channel; this is despite further sublimation diminishing both the inclination of the bubble wall and the possibility of non-line-of-sight secondary electrons. Future observation of the phenomena using backscattered electron imaging, where a line-of-sight between the surface and the detector is assured, would avoid any possible ambiguity. Figure 1c shows the intersection on the left side of the bubble cavity in Figure 1a after a total of 19 min of etching. The location of (what we interpret as) the grain-boundary ridge which was previously relatively central within the etching channel is now located at its bottom edge. This observation strengthens our interpretation that the etching channel follows a path normal to the surface retreating under sublimation with the grain boundary aligned at some different angle. Further etching obscured the location of the ridge entirely (unfortunately no image was saved).

Figure 2 shows examples of two different ice surface preparations undergoing sublimation. Figure 2a–e show a freshly cut surface being etched. This is a sample that has undergone only minimal ( $<5$  min) pre-etching. Before etching, the location of the grain-boundary groove is not easy to discern ( $1\text{--}2\ \mu\text{m}$  across; Fig. 2a). After etching under vacuum at a rate of  $\sim 6\ \mu\text{m}\ \text{min}^{-1}$ , a narrow and shallow etching channel forms during sublimation, but is no longer discernible following the removal of only  $180\ \mu\text{m}$  of ice. The bright spots that develop on the surface due to coagulated impurities, referred to as etching spots (see Fig. 2c–e), give an indication of the length scale of surface roughness features. We note that once the characteristic separation between etching spots exceeds the width of the etching channel (in this example  $10\text{--}20\ \mu\text{m}$ ) it is generally difficult to distinguish the channel from other surface roughness. In contrast, Figure 2f–j show the surface of a specimen cut and left for 3 days at  $-20^{\circ}\text{C}$  at atmospheric pressure (pre-etched) prior to insertion in the SEM. The initial grain-boundary groove has a characteristic width of around  $25\ \mu\text{m}$ , substantially wider (and deeper) than the groove in Figure 2a. On sublimation at a rate of  $\sim 20\ \mu\text{m}\ \text{min}^{-1}$ , the etching channel remains clearly visible even after  $200\ \mu\text{m}$  has been removed from the surface, at which point the characteristic separation between etching peaks is also  $10\text{--}20\ \mu\text{m}$ , but the channel width is  $\sim 50\ \mu\text{m}$ . If rapid sublimation from a grain boundary is the cause of etching grooves or channels then we would certainly expect a channel to be formed and clearly visible on the surface after prolonged etching, except where neighbouring crystalline orientations are almost identical. This is not the case (Fig. 2d and e), and etching channels were only observed to persist on surfaces which had been pre-etched to allow substantial grain-boundary grooves to form on the initial surface prior to rapid sublimation under vacuum. In other words, it is the pre-existence of a groove, not the pre-existence of a grain boundary, that causes further propagation of the groove during sublimation.

The evidence presented in Figures 1 and 2 appears consistent with our explanation of etching-channel formation,

while being hard to reconcile with the interpretation offered by Obbard and others (2006). In particular we note that Obbard and others state that their model explains the ease of detection of grain boundaries on a subliming surface; this is in direct contradiction of the evidence presented in Figure 2, where it quickly becomes impossible to locate the grain boundary or etching channel on a freshly cut surface after sublimation under vacuum. Indeed our interpretation is also consistent with work presented in earlier studies from the same group (e.g. Cullen and Baker, 2001, figs 3 and 4) which clearly show that substantial etching channels are present after prolonged pre-etching (sublimation in the cold room at  $-20^{\circ}\text{C}$  at atmospheric pressure for weeks) while without significant pre-etching, etching channels are not observed.

However, the ice surfaces Obbard and others present (figs 4 and 5 of Obbard and others, 2006) do suggest a grain boundary could be located at the etching channels in their samples, although their preparation conditions are not given. The explanation for this apparent contradiction between our studies and theirs is likely to be related to differences in sample preparation, and the vapour pressures and temperatures experienced by the sample during etching. We note that, to our knowledge, Obbard and co-workers do not in general insert their ice specimens into the SEM at  $-196^{\circ}\text{C}$  but rather at close to the temperature of their cold room. If this is the case, they are unable to control the very rapid sublimation from the ice surface that will occur during the period when the vacuum chamber is evacuated while the ice sample is still warm; this adds an extra layer of complication when interpreting their work.

Obbard and others cite a thermodynamic argument that the sublimation rate at the convex surfaces found at a grain boundary will be more rapid than for a flat surface, as described by Kelvin's equation:

$$\ln(P_0/P_r) = 2\gamma_{\text{vs}}V_m/RT \quad (1)$$

where  $P_0$  is the vapour pressure over a flat surface of ice,  $P_r$  is the pressure over a surface of radius  $r$ ,  $\gamma_{\text{vs}}$  is the vapour–solid interface energy,  $V_m$  is the molar volume of the ice phase,  $R$  is the gas constant and  $T$  the temperature. Kelvin's equation (1) describes the variation in saturation vapour pressure above an ice surface and is useful for describing the formation of a grain-boundary groove under quasi-equilibrium conditions (such as those in the cold room during pre-etching). The surface energies at the grain-boundary–surface interface must balance, thus maintaining a constant contact angle,  $\theta$ , such that:

$$\gamma_{\text{ss}} = 2\gamma_{\text{vs}} \cos(\theta/2). \quad (2)$$

The increased free energy of water molecules at the site of a grain boundary,  $\gamma_{\text{ss}}$ , and the curvature lead to a higher equilibrium vapour pressure over this region according to Equation (1). Indeed the equation and the two-dimensional broken-bond model that Obbard and others (2006) cite support our view that grain-boundary grooves will widen and eventually be lost. They go on to suggest that the etching channel tracks the grain boundary during sublimation despite the above argument because of more rapid sublimation from the higher-energy sites at the boundary. However, the Kelvin equation (1) and increased boundary energy do not complete the picture; it is misleading not to consider the magnitude of the effect. The rate of deposition or sublimation of water vapour to or from the surface,

$\Gamma$  ( $\text{m s}^{-1}$ ), is estimated using the Hertz–Knudsen equation (e.g. Kossacki and others, 1999):

$$\Gamma = \alpha \frac{V_m}{\sqrt{2\pi\mu RT}} (P_{\text{chamber}} - P_{\text{saturation}}), \quad (3)$$

where  $\alpha$  is the uptake or release coefficient ( $\alpha = 1$  if molecules stick or escape perfectly from the surface, which we assume here) and  $\mu$  is the molar mass of ice.  $P_{\text{chamber}}$  is the partial pressure of the water vapour in the vacuum chamber or sealed container in the cold room and  $P_{\text{saturation}}$  is the saturation vapour pressure over the surface of the ice; it is a function of  $T$ ,  $r$  and  $\gamma_{\text{ss}}$ , such that  $P_{\text{saturation}} \approx P_r$  over the grain-boundary groove and  $P_{\text{saturation}} \approx P_0$  elsewhere over the flat surface.

For an ice surface in a sealed container at atmospheric pressure,  $P_{\text{chamber}} \approx P_0$  such that deviations in the saturation vapour pressure over the boundary,  $P_r$ , which result from a grain-boundary groove with angle  $\theta$  at equilibrium, lead to the sublimation of ice from the grain boundary according to Equations (1) and (3). This progressively increases  $r$  and thus reduces the rate of groove formation with time. This is the basis of the pre-etching process. Note also that recent work suggests that, at temperatures close to the melting point, grain-boundary grooves could be formed by surface diffusion through a quasi-liquid layer from the site of the grain boundary on the surface (Style and Worster, 2005).

Ice under vacuum can no longer be considered at equilibrium because, due to the vacuum pump,  $P_{\text{chamber}}$  may be less than  $P_{\text{saturation}}$ . If  $(P_{\text{saturation}} - P_{\text{chamber}}) \gg (P_r - P_0)$  the difference in  $\Gamma$  over grain-boundary grooves relative to the ordinary ice surface will become negligible. In this case the grain-boundary groove will become indistinguishable from the roughness and crystalline facets developed on the surface during sublimation or etching. For example, applying Equations (1) and (3), for an ice surface at  $-80^{\circ}\text{C}$ ,  $P_0 = 0.055$  Pa (Petrenko and Whitworth, 1999) and  $P_{\text{chamber}} \approx 1.3 \times 10^{-4}$  Pa, a narrow grain-boundary groove ( $r = 10$  nm) has a substantially higher sublimation rate over the grain boundary than the flat surface such that  $\Gamma_r/\Gamma_0 = 1.19$  (where  $\Gamma_0 \approx 5 \mu\text{m min}^{-1}$ ). However,  $r$  rapidly increases as a result, and by the time  $r = 1 \mu\text{m}$ ,  $\Gamma_r/\Gamma_0 = 1.002$ , the sublimation rate over the boundary is almost identical to the bulk. We see from Figure 2a–e that after just a few minutes at  $-80^{\circ}\text{C}$  the spacing between surface etching spots is greater than  $1 \mu\text{m}$  such that the grain-boundary groove is no longer easily distinguishable. At  $-60^{\circ}\text{C}$  the values are similar,  $P_0 = 1.08$  Pa, and  $\Gamma_r/\Gamma_0 \approx 1.17$  for  $r = 10$  nm, whereas  $\Gamma_r/\Gamma_0 \approx 1.002$  for  $r = 1 \mu\text{m}$ . On this basis we confirm that the etching channel that develops in Figure 2f–j results from the structure of the initial groove and not differing sublimation rates over the grain boundaries. This simple description is, of course, limited by practical effects such as the coagulation of impurities at the edges of etch channels by surface diffusion. It is also possible that  $\alpha$  will vary for differing crystalline planes, but this will also be intrinsically related to  $P_0$ .

It may still be possible to infer the location of grain boundaries on micrographs from other features, such as a change in the surface texture from differently oriented ice crystals which develop after prolonged etching. Additionally the extremely rapid sublimation rates likely to occur when ice at  $-20^{\circ}\text{C}$  is pumped down to vacuum and cooled to  $-115^{\circ}\text{C}$  simultaneously will lead to complex sublimation processes. These could result in crystalline faceting

dependent on grain orientation similar to that observed by Cross (1969); changes in facet direction would indicate a grain boundary, although its precise location would remain difficult to pinpoint.

In light of these arguments, it is interesting to examine micrographs presented by Obbard and others previously. For example, figure 2 of Obbard and others (2003) shows no sign of an etch channel despite sublimation at  $-95^{\circ}\text{C}$  for 60 min (which we estimate removed  $\sim 25\ \mu\text{m}$  of ice, though the actual amount may have been higher if the specimen temperature was not well constrained). Figure 5a of Obbard and others (2003) indicates an etching channel next to a bubble cavity, presumably formed from a grain-boundary groove during the pump down to vacuum. The channel contains two ridges, an upper and lower; the upper ridge, which is surmounted by a coagulated impurity, is cited by the authors as the grain boundary. However, the lower ridge in the channel could equally well represent the location of the grain boundary, and changes in the surface texture would tend to support this interpretation. The impurity ridge might well be the original location of the grain boundary on the surface prior to etching.

In summary, we have presented evidence and arguments that support our original interpretations. That is, etch channels form as a result of sublimation over grain-boundary grooves on the initially cooled ice surface, and the location of the etch channel is not directly related to the location of the grain boundary on the subliming surface. It may be possible that temperature and vapour-pressure combinations different to those used in our studies can lead to grooves located on grain boundaries during sublimation in the SEM. If this is the case, an explicit description of such preparation and sublimation conditions in future publications on the subject would be very useful to other researchers.

British Antarctic Survey,  
Natural Environment  
Research Council,  
Madingley Road,  
Cambridge CB3 0ET, UK

Piers R.F. BARNES\*  
Eric W. WOLFF

Department of Earth Sciences,  
University of Bristol,  
Queen's Road,  
Bristol BS8 1RJ, UK

David C. MALLARD

\*Present address  
CSIRO Industrial Physics  
PO Box 218, Lindfield, Sydney,  
New South Wales 2070, Australia  
E-mail: piers.barnes@csiro.au

7 October 2006

## REFERENCES

- Barnes, P.R.F. and E.W. Wolff. 2004. Distribution of soluble impurities in cold glacial ice. *J. Glaciol.*, **50**(170), 311–324.
- Barnes, P.R.F., R. Mulvaney, E.W. Wolff and K. Robinson. 2002. A technique for the examination of polar ice using the scanning electron microscope. *J. Microsc.*, **205**(2), 118–124.
- Barnes, P.R.F., E. Wolff, D.C. Mallard and H.M. Mader. 2003. SEM studies of the morphology and chemistry of polar ice. *Microsc. Res. Techn.*, **62**(1), 62–69.
- Cross, J.D. 1969. Scanning electron microscopy of evaporating ice. *Science*, **164**(3876), 174–175.
- Cullen, D. and I. Baker. 2001. Observation of impurities in ice. *Microsc. Res. Techn.*, **55**(3), 198–207.
- Kossacki, K.J., W.J. Markiewicz, Y. Skorov and N.I. Kömle. 1999. Sublimation coefficient of water ice under simulated cometary-like conditions. *Planet. Space Sci.*, **47**(12), 1521–1530.
- Obbard, R., D. Iliescu, D. Cullen and I. Baker. 2003. SEM/EDS comparison of polar and seasonal temperate ice. *Microsc. Res. Techn.*, **62**(1), 49–61.
- Obbard, R., I. Baker and D. Iliescu. 2006. Correspondence. Grain boundary grooving in ice in a scanning electron microscope. *J. Glaciol.*, **52**(176), 169–172.
- Petrenko, V.F. and R.W. Whitworth. 1999. *Physics of ice*. Oxford, etc., Oxford University Press.
- Style, R.W. and M.G. Worster. 2005. Surface transport in premelted films with application to grain-boundary grooving. *Phys. Rev. Lett.*, **95**(17), 176102. (10.1103/PhysRevLett.95.176102.)